Journal of
Composites Science

MDPI

Communication

Biogenic Preparation, Characterization, and Biomedical Applications of Chitosan Functionalized Iron Oxide Nanocomposite

Devaraj Bharathi [1,†], Ranjithkumar Rajamani [2,†], Belay Zeleke Sibuh [3], Soumya Pandit [4], Sharad Agrawal [4], Neeraj Mishra [5], Mohit Sahni [6], Vijay Kumar Thakur [7,8,*] and Piyush Kumar Gupta [4,*]

1 Department of Biotechnology, Hindusthan College of Arts and Science, Coimbatore 6410028, India; bharathi.deva@yahoo.in
2 Viyen Biotech LLP, Coimbatore 6410021, India; biotechranjith@gmail.com
3 Department of Biotechnology, School of Engineering and Technology, Sharda University, Greater Noida 201310, India; belayzeleke63@yahoo.com
4 Department of Life Sciences, School of Basic Sciences and Research, Sharda University, Greater Noida 201310, India; soumya.pandit@sharda.ac.in (S.P.); sharad.agrawal@sharda.ac.in (S.A.)
5 Amity Institute of Pharmacy, Amity University, Gwalior 474005, India; neerajdops@gmail.com
6 Department of Physics, School of Basic Sciences and Research, Sharda University, Greater Noida 201310, India; mohit.sahni@sharda.ac.in
7 Biorefining and Advanced Materials Research Centre, Scotland's Rural College (SRUC), Kings Buildings, Edinburgh EH9 3JG, UK
8 School of Engineering, University of Petroleum & Energy Studies (UPES), Dehradun 248007, India
* Correspondence: Vijay.Thakur@sruc.ac.uk (V.K.T.); dr.piyushkgupta@gmail.com (P.K.G.)
† These authors contributed equally to this work.

check for updates

Citation: Bharathi, D.; Rajamani, R.; Sibuh, B.Z.; Pandit, S.; Agrawal, S.; Mishra, N.; Sahni, M.; Thakur, V.K.; Gupta, P.K. Biogenic Preparation, Characterization, and Biomedical Applications of Chitosan Functionalized Iron Oxide Nanocomposite. *J. Compos. Sci.* **2022**, *6*, 120. https://doi.org/10.3390/jcs6050120

Academic Editor: Francesco Tornabene

Received: 27 March 2022
Accepted: 20 April 2022
Published: 22 April 2022

Publisher's Note: MDPI stays neutral with regard to jurisdictional claims in published maps and institutional affiliations.

Abstract: Chitosan (CS) functionalization over nanomaterials has gained more attention in the biomedical field due to their biocompatibility, biodegradability, and enhanced properties. In the present study, CS functionalized iron (II) oxide nanocomposite (CS/FeO NC) was prepared using *Sida acuta* leaf extract by a facile and eco-friendly green chemistry route. Phyto-compounds of *S. acuta* leaf were used as a reductant to prepare CS/FeO NC. The existence of CS and FeO crystalline peaks in CS/FeO NC was confirmed by XRD. FE-SEM analysis revealed that the prepared CS/FeO NC were spherical with a 10–100 nm average size. FTIR analyzed the existence of CS and metal-oxygen bands in the prepared NC. The CS/FeO NC showed the potential bactericidal activity against *E. coli*, *B. subtilis*, and *S. aureus* pathogens. Further, CS/FeO NC also exhibited the dose-dependent anti-proliferative property against human lung cancer cells (A549). Thus, the obtained outcomes revealed that the prepared CS/FeO NC could be a promising candidate in the biomedical sector to inhibit the growth of bacterial pathogens and lung cancer cells.

Keywords: chitosan; FeO; nanocomposite; antibacterial; anticancer

1. Introduction

Nanomaterials have received significance in developing new and different industrial applications due to their unique shape, size, and high surface area to volume ratio [1–3]. In biomedical industries, various approaches have been used to develop a new path to control and prevent microbial infections using novel nanoparticles (NPs). Many literature studies have demonstrated the significant bactericidal properties of NPs against bacterial pathogens [4–6]. However, antibacterial resistance is the key problem in the biomedical field, increasing the severity of bacterial infections that can indicate the requirement of novel antibacterial agents against those drug-resistant and severe infection-causing pathogens. Previous reports revealed that the metallic NPs and NCs could be better alternative antibacterial agents like natural and synthetic antibiotics [7–11]. Different NPs and NCs have been

utilized in the textile coating, cosmetics, food, and paint industries, which interestingly showed a high prospective to solve the antibiotic resistance problem [12–17].

Currently, NPs and NCs synthesized using plants by green chemistry route have been received the focus of interest for their various applications in biological, pharmaceutical, and food industries, because of the unique physicochemical properties, less toxic, eco-friendly, economic, and easy scale-up [18–21]. Iron (II) oxide nanoparticles (FeO NPs) are typically interesting in modern green nanotechnology because of their superparamagnetic properties, high magnetic susceptibility, superior catalytic and bactericidal properties [22,23]. Additionally, researchers have been focusing on the functionalization of CS over FeO NPs to enhance the physio-chemical and biological properties [24].

Among the various natural biopolymers, several researchers have focused on chitosan as a potential functional biomaterial for its biocompatibility, biodegradability, non-toxicity, and bacteriostatic properties [25]. Previous reports demonstrated the chitosan's utilization for surface functionalization of metal and metal oxide NPs [26,27]. Apart from the antibiotic properties, several reports demonstrated the anti-cancer and antioxidant properties of CS and chitosan-functionalized NPs [28,29]. Many studies have revealed that the CS functionalized biomaterials can be prepared as a nanostructured anti-cancer drug carrier [30]. From this significance, the present study aimed to prepare CS/FeO NC using the *Sida acuta* plant. *S. acuta* belongs to the family of Malvaceae and has many pharmacological properties [31]. Further, the prepared CS/FeO NC was characterized and assessed its bactericidal and anti-proliferative properties.

2. Materials and Methods

2.1. Sources and Materials

High-pure chitosan (deacetylation degree: ≥75%, MW: 190–375 kDa), iron (II) sulfate (Purity ≥ 99.0%), and nutrient broth (Quality level = 200) were procured from Sigma-Aldrich. *S. acuta* leaves were collected from the Bharathiar University campus, Coimbatore, and authenticated by BSI (SRC/5/23/2020/650).

2.2. S. acuta Leaf Extraction

Freshly collected leaf parts of *S. acuta* were cleaned with tap water and dried. About 1 g of dried leaf sample was mixed with 100 mL of distilled water and heated at 100 °C for 15 min, and then the extracted solution was filtered and used for the biogenic preparation of CS/FeO NC (Figure 1).

2.3. Biogenic Preparation of CS/FeO NC

CS (0.5 g) was dissolved into 1% (*v*/*v*) acetic acid (50 mL) followed by the addition of 0.5 M iron (II) sulfate (25 mL) and *S. acuta* leaf extract (25 mL), and vigorously stirred under 60 °C for 30 min. Further, the resultant was centrifuged at 12,000 rpm for 10 min and air-dried at 80 °C to obtain the final CS/FeO NC.

2.4. Physicochemical Characterization

The optical, morphological, and chemical properties of CS/FeO NC were characterized by UV-vis spectroscopy (JASCO-V-670), X-ray Diffraction XRD (PANalytical X'pert Pro, Malvern, UK), and field emission-scanning electron microscopy (TESCAN-MIRA3) attached with energy-dispersive X-ray spectroscopy (EDS), and Fourier transform infrared spectroscopy (FTIR-00585, PerkinElmer, New Delhi, India).

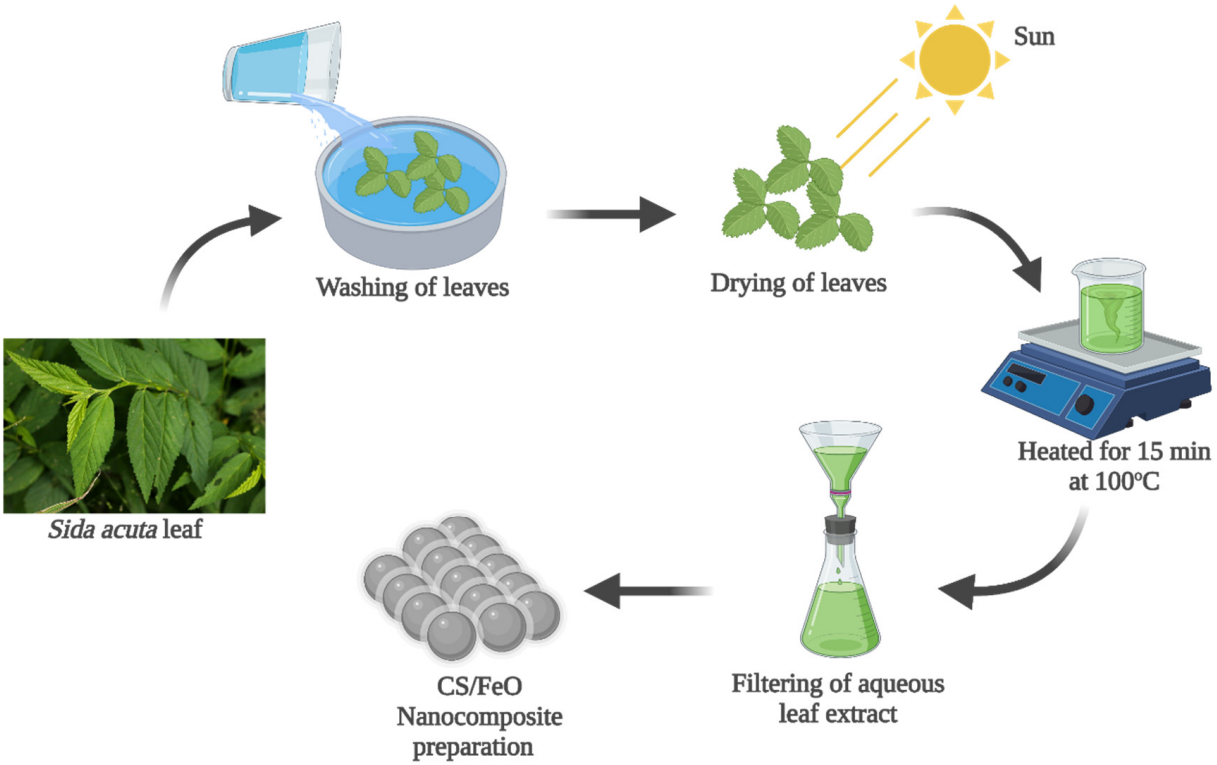

Figure 1. Preparation of *S. acuta* aqueous leaf extract utilized for the biogenic synthesis of CS/FeO nanocomposite.

2.5. Antibacterial Assay

Spectrophotometer turbidimetry technique was used to analyze the antibacterial activity of CS/FeO NC. *S. aureus*, *B. subtilis*, and *E. coli* were used as test bacterial pathogens. Bactericidal properties of CS/FeO NC were evaluated in nutrient broth using the optical density (570 nm) measurement method. The bacterial concentration was diluted to 10^5 CFU/mL. CS/FeO NC was added into the bacterial suspension at a 50 µg/mL concentration and incubated overnight. The bacteriostatic rate (%) was calculated as follows Equation (1),

$$\text{Bacteriostatic rate } (\%) = (\text{control O.D.value} - \text{test sample O.D. value} \div \text{control O.D. value}) \times 100 \quad (1)$$

2.6. Antiproliferative Activity of CS/FeO NC

Antiproliferative property of prepared CS/FeO NC was evaluated by 3-[4, 5–96 dimethylthiazole-2-yl]-2, 5-diphenyltetrazolium bromide (MTT) assay, as demonstrated previously by Seetharaman et al. (2017) [32]. Lung cancer cells (A549) were procured from NCCS, Pune, India, and grown in a medium containing fetal bovine serum (10%) and antibiotics (1%) in a CO_2 incubator under standard conditions. The grown cells (100 µL) at a density of 1×10^3 were loaded on a culture plate and incubated at 37 °C with 5% CO_2 overnight. Then, various concentration of CS/FeO NC (10, 25, 50, 100, 150 and 200 µg/mL) were added into respective wells and re-incubated. After that, the media was replaced with 10 µL of MTT (5 mg/mL) and again incubated. Further, the MTT solution was removed, and 100 µL of DMSO was added and incubated. The absorbance value was measured using a BioRad-680 plate reader at 570 nm, and the viability percentage was calculated Equation (2).

$$\text{Viability } (\%) = \text{Treated cells/Control cells} \times 100 \quad (2)$$

where C is the control cell's value, and T is the value of the treated cell.

Furthermore, inducing apoptosis by CS/FeO NC against A549 cells was studied by AO/EtBr fluorescent staining technique, as demonstrated previously by Bharathi et al. [33].

2.7. Statistical Analysis

All in vitro tests were performed three independent times in triplicates (n = 3), and the obtained data were represented as mean ± standard deviation. The significance level was analyzed at $p < 0.05$.

3. Results

3.1. Fabrication of CS/FeO NC

Biogenic conversion of iron (II) sulfate to CS/FeO NC was initiated by mixing of $FeSO_4$ and CS with *S. acuta* aqueous leaf extract, which also stimulated the color change from yellowish to black, and thus supported the development of CS/FeO NC (Figure 2(Aa)). Similarly, Boudouh et al. (2021) [34] documented the exhibition of black color during the fabrication of FeO NPs. Secondary metabolites present in *S. acuta* leaf extract and free amino, and hydroxyl groups existing in CS might have joined with ferrous ions (Fe^{II}) and formed Fe-ellagate conjugate. Simultaneously, the formed conjugate leads to the nucleation that goes into reverse micellization, which later causes the reduction of Fe^{+} to nano-FeO [35].

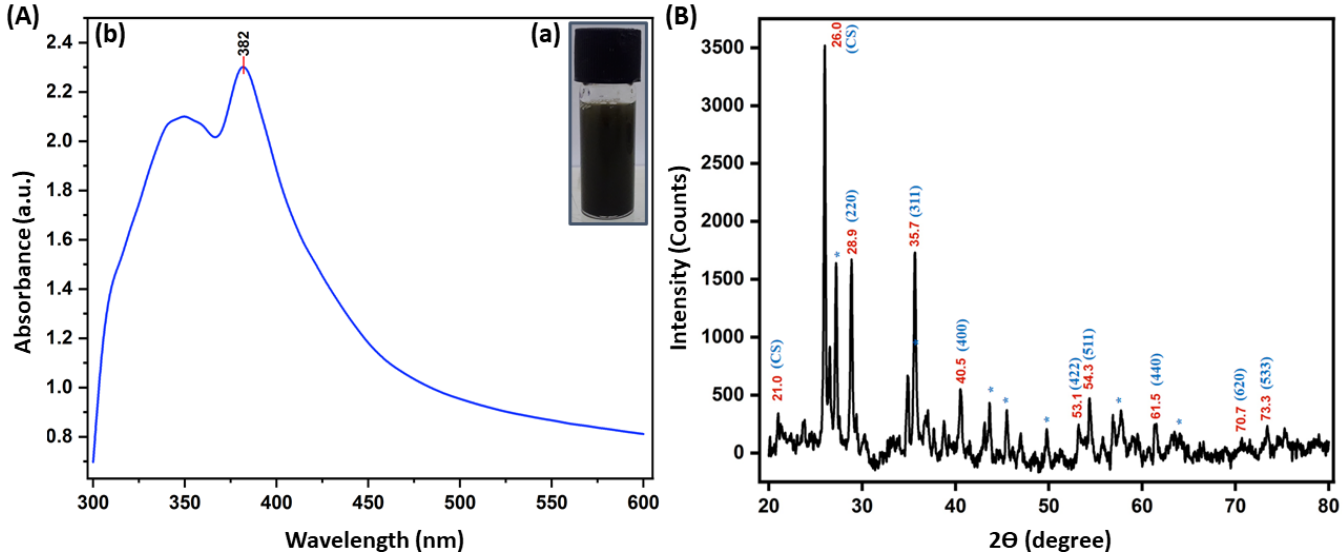

Figure 2. (**Aa**) CS/FeO NC image, (**Ab**) UV-vis spectra, and (**B**) XRD spectra of *S. acuta* leaf extract mediated CS/FeO NC.

3.2. Physicochemical Properties of CS/FeO NC

3.2.1. UV-Visible Spectroscopy Analysis

The optical properties of CS/FeO NC were analyzed by UV-vis spectroscopy. The CS/FeO NC has displayed a maximum absorbance peak at 382 nm (Figure 2(Ab)) and thus indicated a convenient surface plasmon resonance character for FeO nanoparticles. The obtained findings corresponded to Bibi et al. (2019) [36] and Abdullah et al. [37].

3.2.2. XRD Analysis

As shown in Figure 2B, the obtained 2θ peaks around 28.9°, 35.7°, 40.5°, 53.1°, 54.3°, 61.5°, 70.7°, and 73.3° were corresponded to (220), (311), (400), (422), (511), (440), (620) and (533) orientations, which are revealed that the CS/FeO NC are having a typical cubic magnetite crystallite (Fe_3O_4) arrangement and also matched with the JCPDS number # 019-0629 [38]. The obtained other peaks at 2θ = 21.0 and 26.0 may be exhibited due to the CS crystallization over CS/FeO NC and consequently revealed the establishment of organic/inorganic NC. The other peaks may be raised from organic phases in the CS/FeO complex [26]. Further, the crystalline size of CS/FeO NC was calculated using Scherrer's equation, as described previously by [36], and was found to be 18 nm.

3.2.3. FTIR Analysis

The FTIR spectra of CS/FeO NC, CS, *S. acuta* is shown in Figure 3. *S. acuta* IR spectra exhibited free O-H stretching groups at 3728 cm^{-1}, 3609 cm^{-1}, and 948 cm^{-1}, C–H vibrations near 2988 cm^{-1}, 2884 cm^{-1}, 2361 cm^{-1}, 1391 cm^{-1} and 676 cm^{-1}, N–H bands around 1663 cm^{-1}, 1552 cm^{-1}, and C–Br vibrations near 575 cm^{-1}, 530 cm^{-1} and 467 cm^{-1} assigned to the carboxylic, phenolic and amine functional groups present in leaf extract [39,40]. CS FTIR spectra showed a typical amine stretches near 1656 cm^{-1} and 1395 cm^{-1}, hydroxyl bands at 3633 cm^{-1}, 669 cm^{-1}, and 624 cm^{-1}, C-C and C=O vibrations around 1552 cm^{-1}, 941 cm^{-1}, and 903 cm^{-1}, and C–H bands near 844 cm^{-1}, 572 cm^{-1} and 460 cm^{-1} were attributed to the amine groups and acetylated groups of CS [41,42]. CS/FeO NC IR spectra revealed the presence of O–H bands around 1080 cm^{-1}, and 958 cm^{-1}, C–H bands at 2976 cm^{-1}, 2889 cm^{-1}, 1255 cm^{-1} and 1150 cm^{-1}, N-H and C=O bands at 1384 cm^{-1}, Fe–O bands at 689 cm^{-1}, 644 cm^{-1}, 546 cm^{-1}, 487 cm^{-1}, 410 cm^{-1} [43]. Moreover, evaluation of CS/FeO NC with other FTIR showed that certain changes in the band positions and intensity may be attributed to the interface of CS and leaf extract with iron (II) sulfate during the formation of NC. The FTIR results revealed that the existence of those functional groups derived from *S. acuta* leaf and CS might have acted as a reductant for the conversion of iron (II) sulfate to nano FeO.

3.2.4. FE-SEM and EDS Analysis

FESEM analyzed the morphological features of prepared CS/FeO NC. The FE-SEM revealed that the prepared NC was spherical with an average size of 10–100 nm (Figure 4a,b). Following our study, Pérez-Beltrán et al. (2021) [44] demonstrated that the SEM investigation of FeO NPs displayed a spherical shape. The elemental configuration of CS/FeO NC was identified by EDS analysis. EDS showed the peaks of Fe (45.90%) together with O (39.50%), C (7.13%), Na (1.40%), and S (6.07%) (Figure 4c), which obviously confirms the development of CS/FeO NC [45]. Similarly, Bibi et al. (2019) [36] reported the detection of Fe, O, and C elements in the synthesized FeO NPs using *P. granatum*.

3.3. Bactericidal Activity

The bactericidal property of prepared CS/FeO NC was analyzed using the broth dilution technique. As shown in Figure 5A, CS/FeO NC showed remarkable bactericidal properties against *B. subtilis*, *S. aureus*, and *E. coli*. *S. acuta* leaf extract exhibited potential bacteriostatic inhibition against the chosen pathogens, and CS showed moderate inhibition activity. The bactericidal activity was higher in the case of CS/FeO NC compared to that of *S. acuta* and CS. However, prepared CS/FeO NC showed higher ZOI against *E. coil* than *B. subtilis* and *S. aureus*. Similarly, Das et al. (2020) [46] demonstrated that the synthesized FeO NPs exhibited potential bactericidal against *S. aureus*, *P. vulgaris*, and *P. aeruginosa*. The FeO NPs synthesized using leaf extract of *A. spinosus* exhibited bactericidal activity against *E. coli* and *B. subtilis* [47]. The bactericidal activity of CS/FeO NC may be due to cell membrane disruption by the generation of ROS, which causes cell death [33].

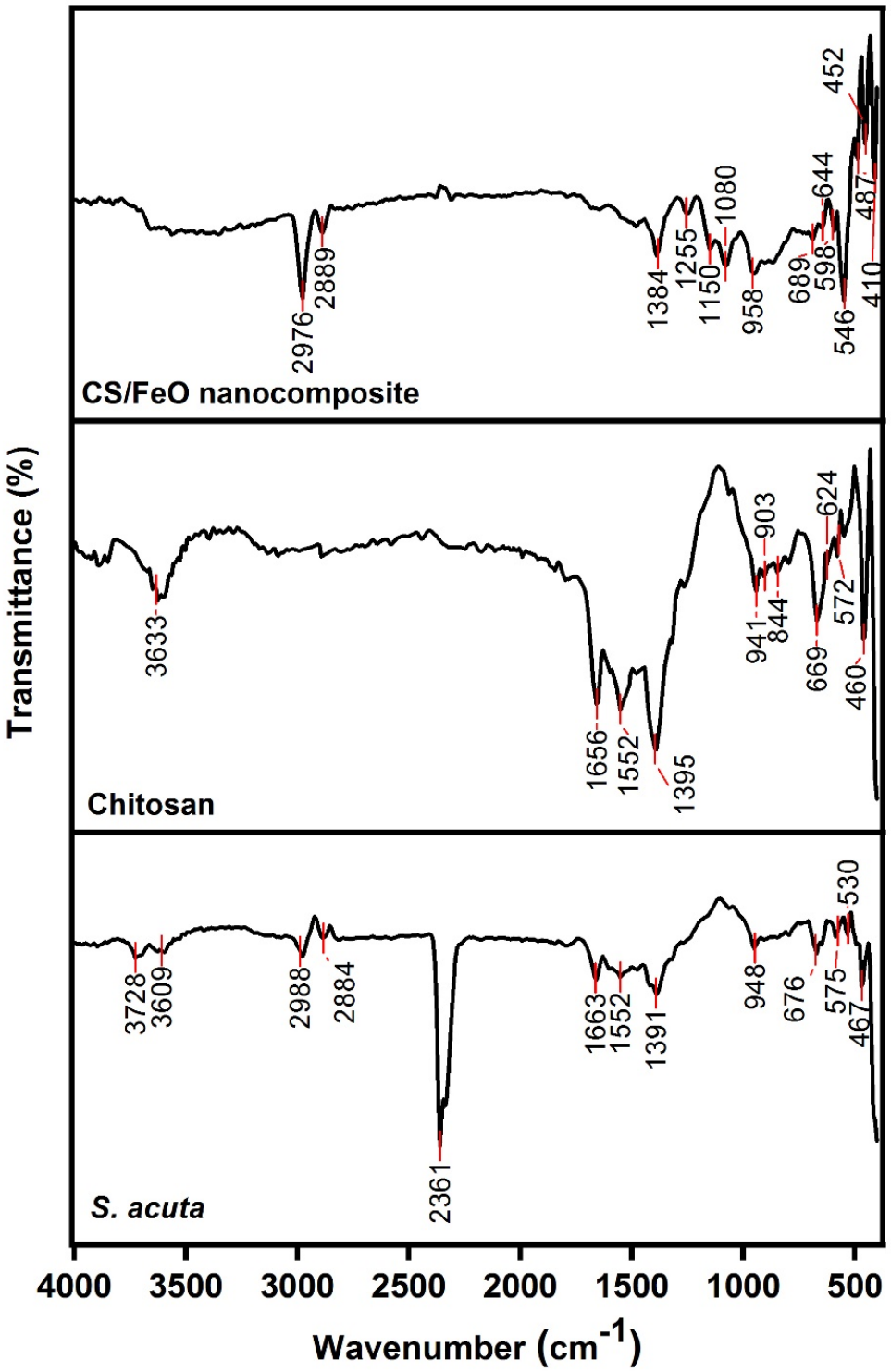

Figure 3. FTIR spectra of CS/FeO NC, CS, and *S. acuta* leaf extract in a wavenumber range of 500–4000 cm^{-1}.

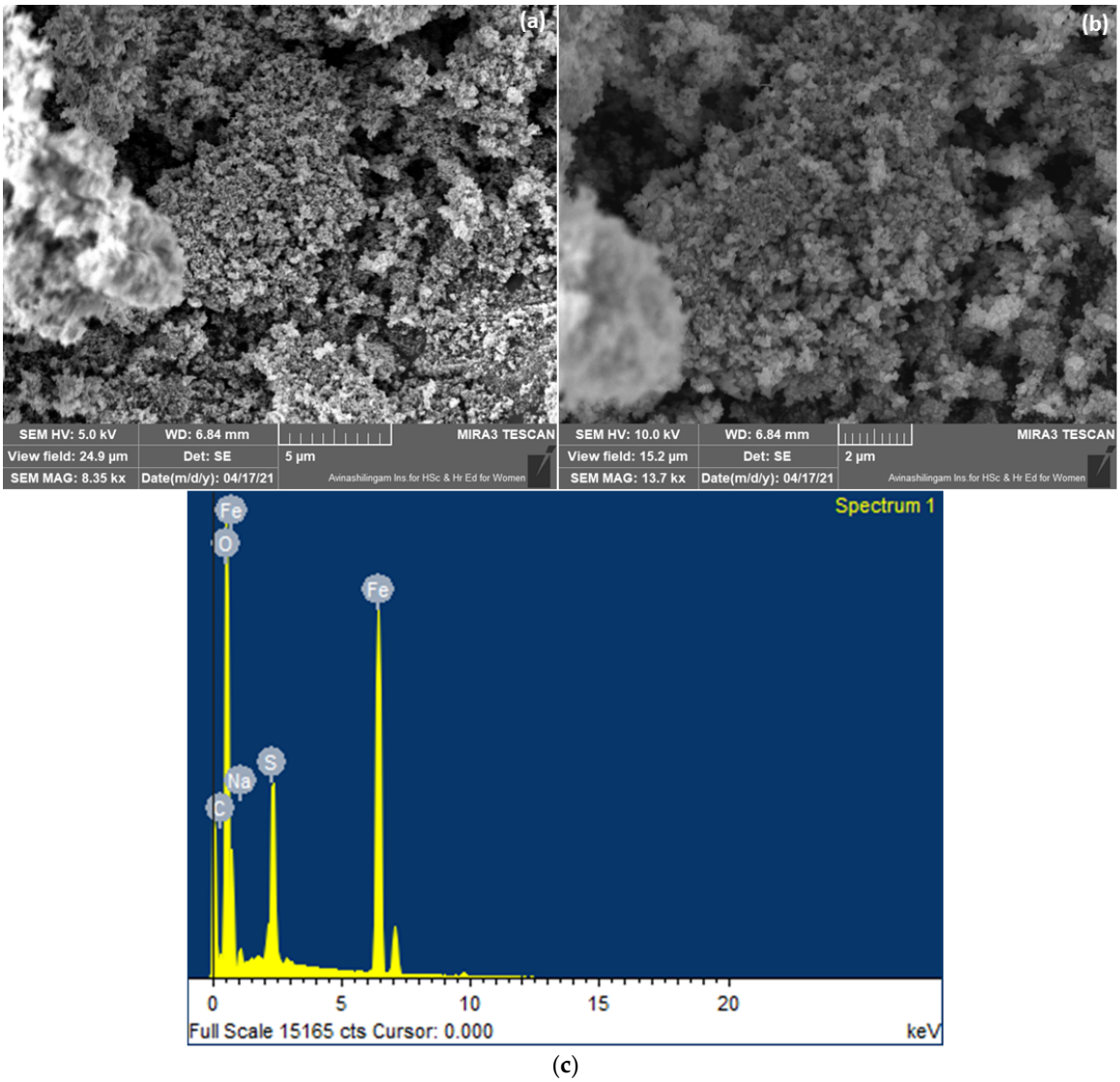

(**c**)

Figure 4. (**a**,**b**) FE-SEM analysis at low and high magnifications, and (**c**) elemental analysis of CS/FeO NC.

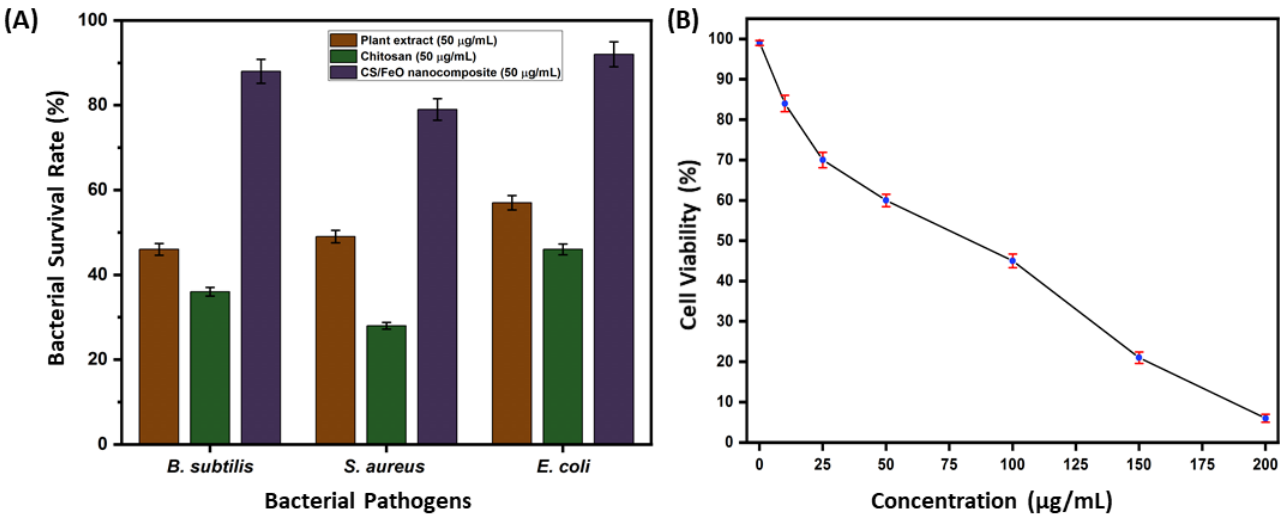

Figure 5. (**A**) Antibacterial activity of CS/FeO NC, CS, and plant extract against *B. subtilis*, *S. aureus*, and *E. coli*. (**B**) In vitro antiproliferative activity of CS/FeO NC against A549 cells.

3.4. Anti-Proliferative Property of CS/FeO NC

The anti-proliferative property of prepared CS/FeO NC was determined by MTT assay against A549 cells. The obtained result revealed that the CS/FeO NC was a concentration-dependent inhibitor for A549 cells (Figure 5B). In our study, 16% inhibition was seen at 10 µg/mL and 94% inhibition was found to be at 200 µg/mL concentration. Prepared CS/FeO NC induced 50% (IC_{50}) of growth suppression property at the concentration of 82 ± 0.50 µg/mL. Similar to our study, biosynthesized silver nanoparticles from *Caulerpa taxifolia* also showed the concentration-dependent anti-lung cancer activity [48]. In addition, the A549 cell proliferation was observed using fluorescence microscopy. Fluorescent microscopic observation of AO/EtBr stained A549 cells is shown in Figure 6a,b. The control cells showed green color, and CS/FeO NC treated cells exhibited red color. The observed, red-colored bodies revealed the cell damage, membrane blebbing, and the presence of apoptotic bodies. Similarly, recent studies demonstrated the anti-cancer properties of FeO-based nanomaterials against various cancer cells [49,50]. The antiproliferative property of CS/FeO NC depends on Fe ions permeability into cells, which induces cell damage, nuclear fragmentation, and apoptosis.

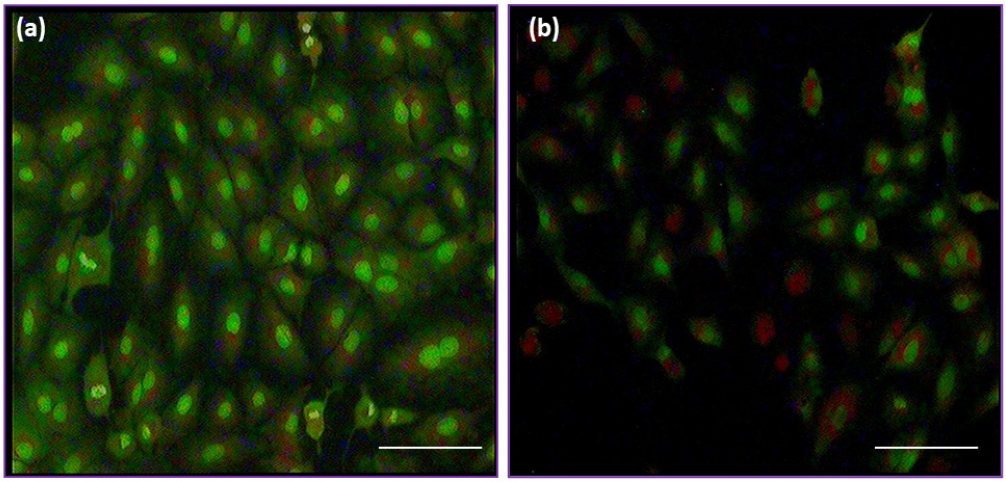

Figure 6. Fluorescence microscopy (40X) images of (**a**) control and (**b**) treated A549 cells.

4. Conclusions

This study has employed an eco-friendly and green chemistry way for the CS/FeO NC preparation. The development of CS/FeO NC has been analyzed by UV-vis, XRD, FE-SEM, EDS, and FTIR. Prepared CS/FeO NC showed remarkable bactericidal properties against *E. coli*, *B. subtilis*, and *S. aureus*. However, CS/FeO NC exhibited higher bactericidal properties against *E. coli* than other pathogens due to the permeability nature of bacterial cells. Furthermore, CS/FeO NC has efficiently suppressed the growth of A549 cells in a concentration-dependent way and stimulated the apoptosis in A549 cells. In conclusion, this study demonstrated that the eco-friendly prepared CS/FeO NC using *S. acuta* leaf could be used as a novel biomaterial to inhibit pathogens and lung carcinoma cells.

Author Contributions: Conceptualization, writing—original draft preparation, writing—review and editing, D.B. and R.R.; writing—review and editing, B.Z.S., S.P., S.A., N.M. and M.S.; supervision, project administration, P.K.G.; funding acquisition, supervision, project administration, V.K.T. and P.K.G. All authors have read and agreed to the published version of the manuscript.

Funding: This research did not receive any specific grant from the funding agencies in the public, commercial, or not-for-profit sectors.

Institutional Review Board Statement: Not Applicable.

Informed Consent Statement: Not Applicable.

Data Availability Statement: The data presented in this study are available on request from the corresponding author.

Conflicts of Interest: The authors declare no competing interests with the work presented in the manuscript.

References

1. Martínez-Ballesta, M.; Gil-Izquierdo, Á.; García-Viguera, C.; Domínguez-Perles, R. Nanoparticles and Controlled Delivery for Bioactive Compounds: Outlining Challenges for New "Smart-Foods" for Health. *Foods* **2018**, *7*, 72. [CrossRef] [PubMed]
2. Bankier, C.; Matharu, R.; Cheong, Y.K.; Ren, G.G.; Cloutman-Green, E.; Ciric, L. Synergistic Antibacterial Effects of Metallic Nanoparticle Combinations. *Sci. Rep.* **2019**, *9*, 16074.
3. Pearce, A.K.; Wilks, T.R.; Arno, M.C.; O'Reilly, R.K. Synthesis and applications of anisotropic nanoparticles with precisely defined dimensions. *Nat. Rev. Chem.* **2021**, *5*, 21–45. [CrossRef]
4. Pal, S.; Tak, Y.K.; Song, J.M. Does the Antibacterial Activity of Silver Nanoparticles Depend on the Shape of the Nanoparticle? A Study of the Gram-Negative Bacterium *Escherichia coli*. *Appl. Environ. Microbiol.* **2007**, *73*, 1712–1720. [CrossRef]
5. Raghunath, A.; Perumal, E. Metal oxide nanoparticles as antimicrobial agents: A promise for the future. *Int. J. Antimicrob. Agents* **2017**, *49*, 137–152. [CrossRef]
6. Gabrielyan, L.; Badalyan, H.; Gevorgyan, V.; Trchounian, A. Comparable antibacterial effects and action mechanisms of silver and iron oxide nanoparticles on Escherichia coli and Salmonella typhimurium. *Sci. Rep.* **2020**, *10*, 13145. [CrossRef]
7. Huh, A.J.; Kwon, Y.J. "Nanoantibiotics": A new paradigm for treating infectious diseases using nanomaterials in the antibiotics resistant era. *J. Control. Release* **2011**, *156*, 128–145. [CrossRef]
8. Fernandez-Moure, J.S.; Evangelopoulos, M.; Colvill, K.; Van Eps, J.; Tasciotti, E. Nanoantibiotics: A new paradigm for the treatment of surgical infection. *Nanomedicine* **2017**, *12*, 1319–1334. [CrossRef]
9. Wnorowska, U.; Fiedoruk, K.; Piktel, E.; Prasad, S.; Sulik, M.; Janion, M.; Daniluk, T.; Savage, P.B.; Bucki, R. Nanoantibiotics containing membrane-active human cathelicidin LL-37 or synthetic ceragenins attached to the surface of magnetic nanoparticles as novel and innovative therapeutic tools: Current status and potential future applications. *J. Nanobiotechnol.* **2020**, *18*, 1–18. [CrossRef]
10. Singh, A.; Gautam, P.K.; Verma, A.; Singh, V.; Shivapriya, P.M.; Shivalkar, S.; Sahoo, A.K.; Samanta, S.K. Green synthesis of metallic nanoparticles as effective alternatives to treat antibiotics resistant bacterial infections: A review. *Biotechnol. Rep.* **2020**, *25*, e00427. [CrossRef]
11. Skóra, B.; Krajewska, U.; Nowak, A.; Dziedzic, A.; Barylyak, A.; Kus-Liśkiewicz, M. Noncytotoxic silver nanoparticles as a new antimicrobial strategy. *Sci. Rep.* **2021**, *11*, 13451.
12. Karthika, V.; AlSalhi, M.S.; Devanesan, S.; Gopinath, K.; Arumugam, A.; Govindarajan, M. Chitosan overlaid Fe_3O_4/rGO nanocomposite for targeted drug delivery, imaging, and biomedical applications. *Sci. Rep.* **2020**, *10*, 1–17. [CrossRef] [PubMed]
13. Diamond, D.M.; Campbell, A.M.; Park, C.R.; Halonen, J.; Zoladz, P.R. The Temporal Dynamics Model of Emotional Memory Processing: A Synthesis on the Neurobiological Basis of Stress-Induced Amnesia, Flashbulb and Traumatic Memories, and the Yerkes-Dodson Law. *Neural Plast.* **2007**, *2007*, 60803. [CrossRef] [PubMed]
14. Yeh, Y.-C.; Huang, T.-H.; Yang, S.-C.; Chen, C.-C.; Fang, J.-Y. Nano-Based Drug Delivery or Targeting to Eradicate Bacteria for Infection Mitigation: A Review of Recent Advances. *Front. Chem.* **2020**, *8*, 286. [CrossRef] [PubMed]
15. Lugani, Y.; Sooch, B.S.; Singh, P.; Kumar, S. Nanobiotechnology applications in food sector and future innovations. In *Microbial Biotechnology in Food and Health*; Elsevier: Amsterdam, The Netherlands, 2020; pp. 197–225.
16. Mustafa, F.; Andreescu, S. Nanotechnology-based approaches for food sensing and packaging applications. *RSC Adv.* **2020**, *10*, 19309–19336. [CrossRef]
17. Gao, W.; Zhang, L. Nanomaterials arising amid antibiotic resistance. *Nat. Rev. Genet.* **2021**, *19*, 5–6. [CrossRef]
18. Singh, J.; Dutta, T.; Kim, K.-H.; Rawat, M.; Samddar, P.; Kumar, P. 'Green' synthesis of metals and their oxide nanoparticles: Applications for environmental remediation. *J. Nanobiotechnol.* **2018**, *16*, 84.
19. Rana, A.; Yadav, K.; Jagadevan, S. A comprehensive review on green synthesis of nature-inspired metal nanoparticles: Mechanism, application and toxicity. *J. Clean. Prod.* **2020**, *272*, 122880. [CrossRef]
20. Dikshit, P.; Kumar, J.; Das, A.; Sadhu, S.; Sharma, S.; Singh, S.; Gupta, P.; Kim, B. Green Synthesis of Metallic Nanoparticles: Applications and Limitations. *Catalysts* **2021**, *11*, 902. [CrossRef]
21. Cittrarasu, V.; Kaliannan, D.; Dharman, K.; Maluventhen, V.; Easwaran, M.; Liu, W.C.; Balasubramanian, B.; Arumugam, M. Green synthesis of selenium nanoparticles mediated from Ceropegia bulbosa Roxb extract and its cytotoxicity, antimicrobial, mosquitocidal and photocatalytic activities. *Sci. Rep.* **2021**, *11*, 1032. [CrossRef]
22. Ezealigo, U.S.; Ezealigo, B.N.; Aisida, S.O.; Ezema, F.I. Iron oxide nanoparticles in biological systems: Antibacterial and toxicology perspective. *JCIS Open* **2021**, *4*, 100027. [CrossRef]
23. Roy, S.D.; Das, K.C.; Dhar, S.S. Conventional to green synthesis of magnetic iron oxide nanoparticles; its application as catalyst, photocatalyst and toxicity: A short review. *Inorg. Chem. Commun.* **2021**, *134*, 109050.
24. Alkahtane, A.A.; Alghamdi, H.A.; Aljasham, A.T.; Alkahtani, S. A possible theranostic approach of chitosan-coated iron oxide nanoparticles against human colorectal carcinoma (HCT-116) cell line. *Saudi J. Biol. Sci.* **2021**, *29*, 154–160. [CrossRef] [PubMed]

25. Shanmuganathan, R.; Edison, T.N.J.I.; LewisOscar, F.; Kumar, P.; Shanmugam, S.; Pugazhendhi, A. Chitosan nanopolymers: An overview of drug delivery against cancer. *Int. J. Biol. Macromol.* **2019**, *130*, 727–736. [CrossRef]
26. Bharathi, D.; Ranjithkumar, R.; Vasantharaj, S.; Chandarshekar, B.; Bhuvaneshwari, V. Synthesis and characterization of chitosan/iron oxide nanocomposite for biomedical applications. *Int. J. Biol. Macromol.* **2019**, *132*, 880–887. [CrossRef]
27. Nandana, C.N.; Christeena, M.; Bharathi, D. Synthesis and Characterization of Chitosan/Silver Nanocomposite Using Rutin for Antibacterial, Antioxidant and Photocatalytic Applications. *J. Clust. Sci.* **2021**, *33*, 269–279. [CrossRef]
28. Madhan, G.; Begam, A.A.; Varsha, L.V.; Ranjithkumar, R.; Bharathi, D. Facile synthesis and characterization of chitosan/zinc oxide nanocomposite for enhanced antibacterial and photocatalytic activity. *Int. J. Biol. Macromol.* **2021**, *190*, 259–269. [CrossRef]
29. Priya, K.; Vijayakumar, M.; Janani, B. Chitosan-mediated synthesis of biogenic silver nanoparticles (AgNPs), nanoparticle characterisation and in vitro assessment of anticancer activity in human hepatocellular carcinoma HepG2 cells. *Int. J. Biol. Macromol.* **2020**, *149*, 844–852. [CrossRef]
30. He, C.; Guo, Y.; Karmakar, B.; El-Kott, A.; Ahmed, A.E.; Khames, A. Decorated silver nanoparticles on biodegradable magnetic chitosan/starch composite: Investigation of its cytotoxicity, antioxidant and anti-human breast cancer properties. *J. Environ. Chem. Eng.* **2021**, *9*, 106393. [CrossRef]
31. Benjumea, D.M.; Gómez-Betancur, I.C.; Vásquez, J.; Alzate, F.; García-Silva, A.; Fontenla, J.A. Neuropharmacological effects of the ethanolic extract of Sida acuta. *Rev. Bras. Farm.* **2016**, *26*, 209–215. [CrossRef]
32. Seetharaman, P.; Chandrasekaran, R.; Gnanasekar, S.; Mani, I.; Sivaperumal, S. Biogenic gold nanoparticles synthesized using *Crescentia cujete* L. and evaluation of their different biological activities. *Biocatal. Agric. Biotechnol.* **2017**, *11*, 75–82. [CrossRef]
33. Bharathi, D.; Preethi, S.; Abarna, K.; Nithyasri, M.; Kishore, P.; Deepika, K. Bio-inspired synthesis of flower shaped iron oxide nanoparticles (FeONPs) using phytochemicals of Solanum lycopersicum leaf extract for biomedical applications. *Biocatal. Agric. Biotechnol.* **2020**, *27*, 101698. [CrossRef]
34. Boudouh, D.; Hamana, D.; Metselaar, H.S.C.; Achour, S.; Chetibi, L.; Akhiani, A.R. Low-temperature green route synthesis of Fe_3O_4-C nanocomposite using Olive Leaves Extract. *Mater. Sci. Eng. B* **2021**, *271*, 115276. [CrossRef]
35. Nava, O.J.; Luque, P.; Gómez-Gutiérrez, C.; Vilchis-Nestor, A.; Castro-Beltrán, A.; Mota-González, M.; Olivas, A. Influence of Camellia sinensis extract on Zinc Oxide nanoparticle green synthesis. *J. Mol. Struct.* **2017**, *1134*, 121–125. [CrossRef]
36. Bibi, I.; Nazar, N.; Ata, S.; Sultan, M.; Ali, A.; Abbas, A.; Jilani, K.; Kamal, S.; Sarim, F.M.; Khan, M.I.; et al. Green synthesis of iron oxide nanoparticles using pomegranate seeds extract and photocatalytic activity evaluation for the degradation of textile dye. *J. Mater. Res. Technol.* **2019**, *8*, 6115–6124. [CrossRef]
37. Abdullah, J.A.A.; Eddine, L.S.; Abderrhmane, B.; Alonso-González, M.; Guerrero, A.; Romero, A. Green synthesis and characterization of iron oxide nanoparticles by pheonix dactylifera leaf extract and evaluation of their antioxidant activity. *Sustain. Chem. Pharm.* **2020**, *17*, 100280. [CrossRef]
38. Rusianto, T.; Wildan, M.W.; Abraha, K. Various sizes of the synthesized Fe_3O_4 nanoparticles assisted by mechanical vibrations. *Indian J. Eng. Mater. Sci.* **2015**, *22*, 175–180.
39. Sathiyavimal, S.; Vasantharaj, S.; Bharathi, D.; Saravanan, M.; Manikandan, E.; Kumar, S.S.; Pugazhendhi, A. Biogenesis of copper oxide nanoparticles (CuONPs) using Sida acuta and their incorporation over cotton fabrics to prevent the pathogenicity of Gram negative and Gram positive bacteria. *J. Photochem. Photobiol. B Biol.* **2018**, *188*, 126–134. [CrossRef]
40. Idrees, M.; Batool, S.; Kalsoom, T.; Raina, S.; Sharif, H.M.A.; Yasmeen, S. Biosynthesis of silver nanoparticles using Sida acuta extract for antimicrobial actions and corrosion inhibition potential. *Environ. Technol.* **2019**, *40*, 1071–1078. [CrossRef]
41. Hussein, M.A.M.; Baños, F.G.D.; Grinholc, M.; Dena, A.S.A.; El-Sherbiny, I.M.; Megahed, M. Exploring the physicochemical and antimicrobial properties of gold-chitosan hybrid nanoparticles composed of varying chitosan amounts. *Int. J. Biol. Macromol.* **2020**, *162*, 1760–1769. [CrossRef]
42. Lunkov, A.; Shagdarova, B.; Konovalova, M.; Zhuikova, Y.; Drozd, N.; Il'ina, A.; Varlamov, V. Synthesis of silver nanoparticles using gallic acid-conjugated chitosan derivatives. *Carbohydr. Polym.* **2020**, *234*, 115916. [CrossRef] [PubMed]
43. Soto-Robles, C.A.; Luque, P.A.; Gómez-Gutiérrez, C.M.; Nava, O.; Vilchis-Nestor, A.R.; Lugo-Medina, E.; Ranjithkumar, R.; Castro-Beltrán, A. Study on the effect of the concentration of Hibiscus sabdariffa extract on the green synthesis of ZnO nanoparticles. *Results Phys.* **2019**, *15*, 102807. [CrossRef]
44. Pérez-Beltrán, C.H.; García-Guzmán, J.J.; Ferreira, B.; Estévez-Hernández, O.; López-Iglesias, D.; Cubillana-Aguilera, L.; Link, W.; Stănică, N.; da Costa, A.M.R.; Palacios-Santander, J.M. One-minute and green synthesis of magnetic iron oxide nanoparticles assisted by design of experiments and high energy ultrasound: Application to biosensing and immunoprecipitation. *Mater. Sci. Eng. C* **2021**, *123*, 112023. [CrossRef]
45. Rajiv, P.; Bavadharani, B.; Kumar, M.N.; Vanathi, P. Synthesis and characterization of biogenic iron oxide nanoparticles using green chemistry approach and evaluating their biological activities. *Biocatal. Agric. Biotechnol.* **2017**, *12*, 45–49. [CrossRef]
46. Das, S.; Diyali, S.; Vinothini, G.; Perumalsamy, B.; Balakrishnan, G.; Ramasamy, T.; Dharumadurai, D.; Biswas, B. Synthesis, morphological analysis, antibacterial activity of iron oxide nanoparticles and the cytotoxic effect on lung cancer cell line. *Heliyon* **2020**, *6*, e04953. [CrossRef]
47. Muthukumar, H.; Matheswaran, M. Amaranthus spinosus leaf extract mediated FeO nanoparticles: Physiochemical traits, photocatalytic and antioxidant activity. *ACS Sustain. Chem. Eng.* **2015**, *3*, 3149–3156. [CrossRef]

48. Zhang, D.; Ramachandran, G.; Mothana, R.A.; Siddiqui, N.A.; Ullah, R.; Almarfadi, O.M.; Rajivgandhi, G.; Manoharan, N. Biosynthesized silver nanoparticles using Caulerpa taxifolia against A549 lung cancer cell line through cytotoxicity effect/morphological damage. *Saudi J. Biol. Sci.* **2020**, *27*, 3421–3427. [CrossRef]
49. Rajendran, A.; Alsawalha, M.; Alomayri, T. Biogenic synthesis of husked rice-shaped iron oxide nanoparticles using coconut pulp (*Cocos nucifera* L.) extract for photocatalytic degradation of Rhodamine B dye and their in vitro antibacterial and anticancer activity. *J. Saudi Chem. Soc.* **2021**, *25*, 101307. [CrossRef]
50. Aswini, R.; Murugesan, S.; Kannan, K. Bio-engineered TiO2 nanoparticles using Ledebouria revoluta extract: Larvicidal, histopathological, antibacterial and anticancer activity. *Int. J. Environ. Anal. Chem.* **2020**, *101*, 1–11. [CrossRef]